

Diamond Detectors for Heavy Ion Measurements

E. Berdermann*, K. Blasche, P. Moritz, H. Stelzer

*Gesellschaft für Schwerionenforschung mbH, Planckstraße. 1,
D-64291 Darmstadt, Germany*

and F. Zeytouni

*Institut für Kernphysik der Johann Wolfgang Goethe-Universität Frankfurt am Main,
August-Euler-Straße 6, D-60486 Frankfurt /M, Germany*

Abstract

In 1999, the accelerator facility at GSI is scheduled to deliver beam intensities of about 10^{10} particles/spill for all available ions up to ^{238}U . This necessitates the development of a new generation of radiation-resistant and ultra-fast detectors, in conjunction with new high-speed and low-noise electronics. Preliminary results confirm the suitability of CVD-diamond detectors for both, beam diagnostics, and heavy-ion experiments with projectiles in the energy region from 50 MeV/amu to 2 GeV/amu. Various test measurements with ^{241}Am - α -particles, ^{20}Ne , ^{40}Ca , ^{208}Pb and ^{238}U projectiles and different diamond samples are presented. The measurements demonstrate the excellent timing properties of CVD diamond which result in a unique single-pulse time resolution as well as an extremely high counting-rate capability of diamond detectors. It is shown that the disadvantage of the presently used polycrystalline material with respect to the pulse-height resolution does not prevent the usage of diamond detectors in a wide field of heavy-ion applications.

- ♣ Invited talk given at the XXXVI International Winter Meeting on Nuclear Physics, Bormio 1998

1. Introduction

In 1999 the high-current injector of the synchrotron accelerator SIS at GSI-Darmstadt will deliver ion beams with increased intensities up to the incoherent space charge limit of the SIS. Even for the heaviest ions accelerated, intensities above 10^{10} particles/spill are expected (Figure 1). Absolute particle fluxes have to be known with an accuracy of a few percent in order to optimize the efficiency of particle extraction and beam transport, to determine the cross sections of nuclear reactions as well as the precise spatial dosimetry for the GSI tumor-therapy program.

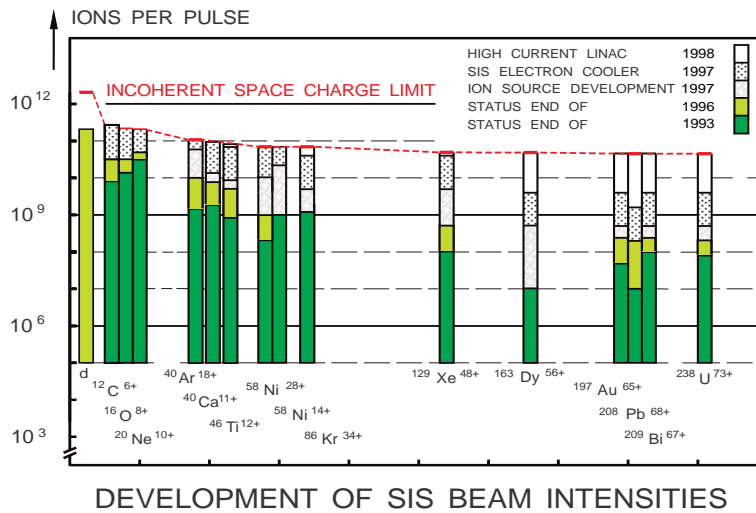


Figure 1: Beam intensities from the high-current injector in the next years

To cope with the very high particles rates, new radiation hard and fast detectors have to be developed in conjunction with new low-noise, high-speed electronics. The most promising detector material with an appropriate characteristic is polycrystalline CVD diamond. Table I lists the relevant material parameters and compares them to silicon.

Table I Basic properties of intrinsic diamond and silicon

Physical Properties at 300 K	Diamond	Silicon
atomic charge	6	14
mass density [$\text{g}\cdot\text{cm}^{-3}$]	3.5	2.33
lattice constant [\AA]	3.57	5.43
band gap [eV]	5.45	1.12
intrinsic carrier density [cm^{-3}]	$< 10^3$	1.5×10^{10}
energy to create e-h pair [eV]	13	3.6
energy to remove an atom from the lattice [eV]	80	28
thermal conductivity [$\text{W cm}^{-1} \text{K}^{-1}$]	20	1.27
thermal expansion coefficient [K^{-1}]	0.8×10^{-6}	2.6×10^{-6}
resistivity [$\Omega \text{ cm}$]	$> 10^{11}$	2.3×10^5
breakdown field [V/cm]	10^7	3×10^5
electron mobility [cm^2/Vs]	2200	1500
hole mobility [cm^2/Vs]	1600	600
saturation velocity [km/s]	220	82
dielectric constant	5.7	11.9

The material parameters of CVD diamond let us expect unique properties of diamond detectors and a favourably low-background implementation in heavy ion experiments due to its lower nuclear charge and mass. The similarity of carbon with human tissue is a particular advantage for the application in the heavy-ion dosimetry, necessary for the tumor-therapy project at GSI [1].

The extremely large band gap of 5.45 eV leads to a very low intrinsic carrier density which at room temperature is by seven orders of magnitude smaller than the intrinsic carrier density of silicon. Consequently the material allows the development of low-noise, solid-state detectors without the need of p-n junction or cooling. The high electron and hole mobilities in conjunction with high breakdown fields lead to ultra-fast counters. The energy needed to remove a carbon atom from the diamond lattice is with 80 eV about three times higher than in the case of silicon. This parameter and the very high thermal conductivity, which is five times higher than for copper, are the reason for the good radiation hardness of CVD-diamond detectors.

2. The CVD Diamond Material

2. 1. Production

The chemical vapour deposition (CVD) synthesis technique for diamond is based on the decomposition of gaseous hydrocarbon molecules, usually methane [2]. In CVD-diamond reactors a gas mixture containing 98% hydrogen and about 1% to 2% methane enters a high-temperature or energetic region in which the gas is activated. Due to the high activation energy necessary for the decomposition of methane the gas mixture must be activated by thermal or microwave-plasma assisted processes.

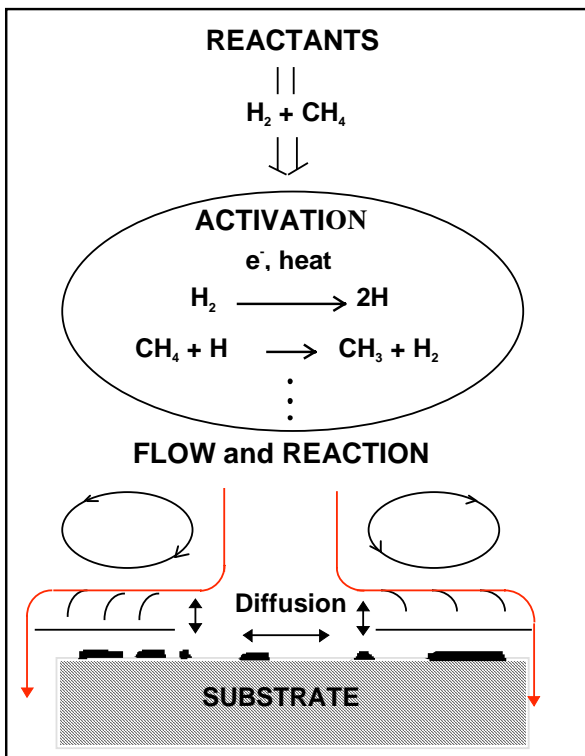


Figure 2: Schematic of the processes in a diamond CVD reactor.

The reactants (methane in hydrogen) are activated by a plasma, undergo gaseous reactions, and are transported to the deposition surface. At the substrate, surface and bulk reactions and diffusion occur, leading to the nucleation, growth, and reaction of both diamond and non diamond carbons [2].

In this region the initial chemical reactions are the decomposition of molecular hydrogen into atomic hydrogen and the formation of methyl radicals. The ability of the atomic hydrogen and the methyl radicals to be transported to a heated substrate defines the growth rate. The transport of atomic hydrogen in a mixture of atomic and molecular hydrogen, its recombination length, lifetime, and drift distance depends on the process parameters such as temperature and pressure. The diamond growth has to take place at moderate temperatures between 500 °C and 1200 °C. Growth at temperatures above or below this range often leads to graphite deposits [2].

Two processes are involved in the growth of diamond. The first is carbon deposition primarily in the form of graphite with a small amount of diamond, the second is selective gasification of graphite by atomic hydrogen. The deposition of diamond can only be realized because diamond has a higher stability towards atomic hydrogen than graphite.

The best quality CVD-diamond material would grow on a diamond substrate since the crystal structure and the lattice constant of 3.57 Å are the same. Apart from this ideal situation many other substrates have been found to accommodate polycrystalline diamond in heteroepitaxial processes. The most common is silicon. A SiC layer with a lattice constant of 4.45 Å is building up as an interface, matching the lattice constant of 5.43 Å of the silicon substrate to the lattice constant of diamond. From this layer small diamond grains start to grow with a columnar shape (Figure 3) up to several millimeters height. Depending on the thickness of the sample the grains achieve edges of a length well above 50 µm on the growth side (Figure 4).

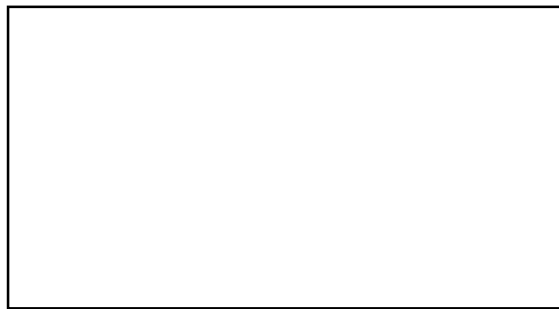


Figure 3: Laser cut edge of a 150 µm thick CVD-diamond sample. The columnar growth of single diamond crystals as well as the stopped growth of some of them are clearly visible.



Figure 4: *Top view of the growth side of a 150 μm thick CVD-diamond detector. The magnification factor shown in this figure is about 200.*

2.2. Characterisation Parameters

In thermal equilibrium the continuously generated charge carriers in a solid state detector are balanced by the recombination processes in which electrons and holes annihilate each other. Traversing charged particles produce excess charge carriers in the detector. The material relaxes towards the equilibrium state and the concentrations of excess electrons and holes decay to their equilibrium values.

The parameter which defines the quality of CVD-diamond detectors is the lifetime of the excess charge carriers in the diamond bulk. Two independent recombination processes with different lifetimes take place [3]. Long living intrinsic transitions from the valence band to the conduction band of the order 10^{-6} s to 1s [4] and extrinsic transitions to recombination centers occupying intermediate states in the band gap with lifetimes of the order of 10^{-8} s to 10^{-10} s [5]. The average lifetime τ is given by Mattiessen's rule (1)

$$1/\tau = 1/\tau_{\text{intrinsic}} + 1/\tau_{\text{extrinsic}} \quad (1)$$

Consequently, τ is dominated by the extrinsic transitions. The finite lifetime of the excess carriers due to structural defects or chemical impurities of the bulk material lead to an incomplete charge collection [3][6][7][8] which is described by the mean free path of the carriers in the bulk, the charge collection distance d_{cd} (2)

$$d_{\text{cd}} = \mu \cdot E_D \cdot \tau \quad (2)$$

with $\mu = \mu_e + \mu_h$, the mobility of electrons and holes
 E_D the applied electric field and
 τ the carrier lifetime.

A minimum ionizing particle produces only 36 e-h pairs in 1 μm CVD diamond [6]. A high quality material of long carrier lifetime and consequently large collection distance is always needed for diamond detectors used in measurements of such particles. The highest quality material available today has a collection distance of 250 μm and a lifetime of the charge carriers of 1 ns. The characterisation for this 1098 μm thick and polished sample is performed with electrons of ≈ 3 MeV from a ^{90}Sr source and with an applied electric field to the detector of $E_D = 1$ V/ μm [6].

A nickel ion of 300 MeV/amu produces 7×10^4 e-h pairs per 1 μm diamond and a uranium ion of the same velocity 8×10^5 e-h pairs per 1 μm diamond. Accordingly, measurements with heavy ions require not necessarily detectors with long carrier lifetimes. As long as the achieved signal amplitudes are well above the electronic threshold a shorter lifetime could be of advantage especially for heavy-ion time measurements [7].

2.3. Irradiation Studies

The tightly bound lattice structure and the high thermal conductivity of diamond suggests that it is insensitive to large doses of radiation. Damages are

indicated by the increase of the dark current and by the decrease of the charge collection distance which implies a decrease of the signal pulse height. The radiation hardness of diamond detectors has been extensively tested during the last 3 years by the RD42 Diamond Collaboration [9] with 5.5 MeV α -particles, different minimum ionizing particles, fast neutrons and with soft γ -rays [6][10].

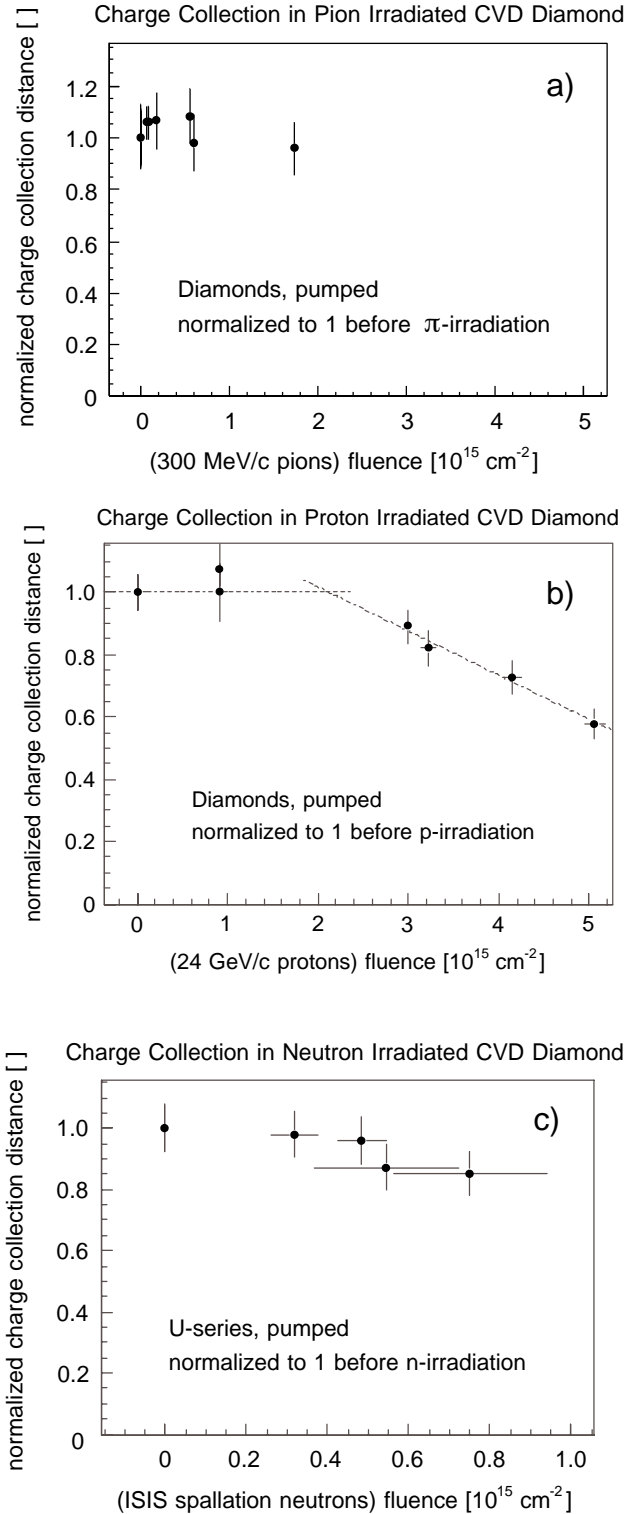


Figure 5:

The charge collection distance in diamond after irradiation with
 a) 300 MeV/c pions,
 b) 24 GeV/c protons,
 c) 1 MeV neutrons as a function of the particle fluence, measured in [particles/cm²].

The "pumped state" refers to an established observation that the charge collection distance at constant bias on the detector increases by a factor of 2 under illumination with γ or β radiation. Above an absorbed dose of 10 Gy the collection distance stays constant [6].

Figure 5 shows recently published data from irradiations with 300 MeV/c pions at the PSI, Villigen, Switzerland, with 24 GeV/c protons at the Proton Synchrotron (PS) at CERN, and with fast neutrons from the ISIS spallation source at the Appleton Laboratory, England.

After pion irradiation no degradation of the charge amplitude was observed up to $1.7 \times 10^{15} \pi/\text{cm}^2$. Under proton irradiation a stable pulse height is found up to $2 \times 10^{15} \text{ p}/\text{cm}^2$. However, above this value the collection distance decreases with a constant slope of $-14\%/10^{15} \text{ p}/\text{cm}^2$ [6]. Neutrons from the ISIS spallation source were used to study diamond detector damages from neutrons with a kinetic energy spectrum peaking at 1 MeV. A weak decrease of the charge amplitude occurs, but the charge collection distance remains within the measurement error up to a fluence of $8 \times 10^{14} \text{ n}/\text{cm}^2$ [6].

In measurements with alpha particles of $E_\alpha = 5 \text{ MeV}$, which are stopped in 12 μm diamond, no change in the gain was found up to a fluence of $10^{13} \alpha/\text{cm}^2$ [10]. The irradiations with 1.2 and 1.3 MeV photons from a ^{60}Co source have shown the curious effect of an increasing collection distance ("the pumping") at doses up to 10 Gy and a saturation of the charge amplitude above this value up to an applied dose of 10 MRad [10].

The highest fluence of heavy ions applied so far to a diamond detector was $5 \times 10^{10}/\text{cm}^2$ uranium ions of 1 GeV/amu. No pulse height degradation was observed on the two irradiated diamond samples. A silicon pin diode irradiated in parallel to the diamond detectors was completely destroyed by this heavy-ion fluence.

3. The CVD-Diamond Detector

It is sufficient to apply electrical contacts to a diamond sample to use it as a particle counter. The large band gap eliminates the need of a p-n junction.

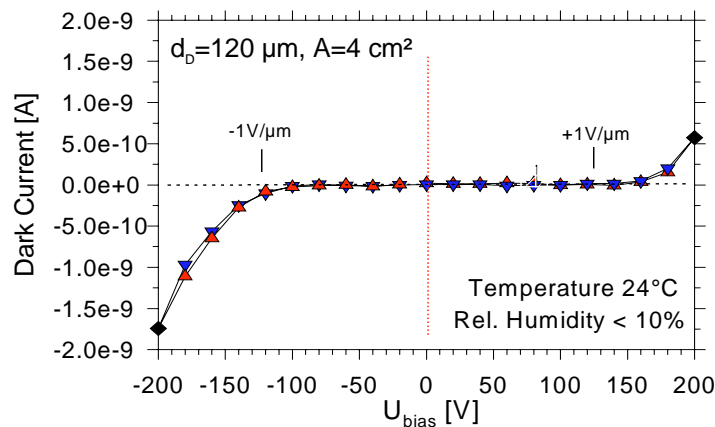


Figure 6: *I-U characteristic of a 120 μm thick diamond detector of an area of 4cm^2 measured with a Keithley 6517 electrometer.*

Chromium-Gold or Titanium-Chromium-Gold electrodes made by evaporation or sputtering are the most common metallisations. Good CVD-diamond detectors have a symmetric I-U behaviour and can therefore be biased

positively or negatively. Figure 6 shows a characteristic I-U curve of a diamond detector measured with an electrometer. Deviations from a symmetric curve indicate inhomogeneously distributed donor and acceptor traps in the bulk or blocking contacts [3]. Ohmic contacts are identified as a linear I-U behaviour above the break-down field on both ends of a completely symmetric curve. Most samples tested have higher break-down fields than the one shown in Figure 6. A common range is from 2 to 6 V/ μm . However, a wide bias range implies a high chemical purity but not necessarily a good charge collection efficiency of the sample. Consequently, this preliminary observation indicates that the incomplete charge collection in diamond detectors must be on account of the polycrystalline CVD-diamond structure.

The collected charge is expected to stay constant at saturated charge carrier velocities over a certain electric field [3]. The rise of the collected charge measured by increasing the bias relates to the ionisation density in the detector.

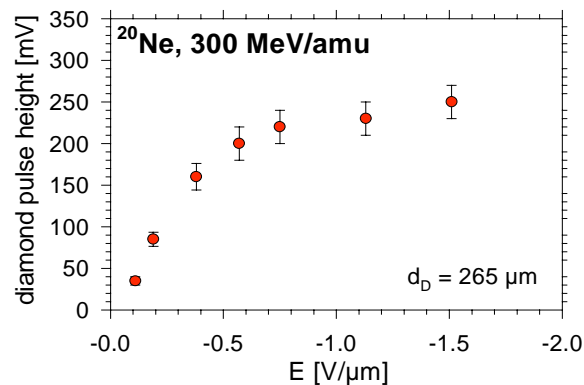


Figure 7: Electric field dependence of the collected charge, measured with ^{20}Ne projectiles of 300 MeV/amu kinetic energy.

For minimum ionizing particles with $Z=1$ an electric field of ± 0.8 V/ μm to ± 1 V/ μm is required to achieve a constant amplitude [6]. Depending on the nuclear charge of the traversing particle the electric field strength has to be higher. Figure 7 shows that an electric field higher than $E_D = -1.5$ V/ μm is required for neon ions with $Z=10$.

4. Pulse-Height Measurements

4.1. Pulse-Height Measurements with Charge-Sensitive Amplifiers

In an experiment in March '96 a 420 μm thick diamond detector was irradiated with ^{20}Ne ions of 300 MeV/amu. A silicon pin-diode was placed behind the diamond counter and both were aligned perpendicular to the beam axis. Figure 8 shows the fragmentation of the ^{20}Ne projectiles in an iron target. The pulse height measured with the pin diode is plotted versus that of the diamond detector. All fragments from $Z=9$ to $Z=4$ are visible. Lighter particles such as alphas and protons are below the adjusted electronic threshold.

The projectile fragmentation process, measured with a diamond-silicon detector setup, allows an on line calibration of the diamond pulse height in MeV^{Silicon} and therefore in charge. The most probable values of the charge distributions



from Figure 8 are plotted in Figure 9. The charge amplitude measured in a second run with calcium ions ($Z=20$) of a slightly higher velocity of 500 MeV/amu is plotted in addition.

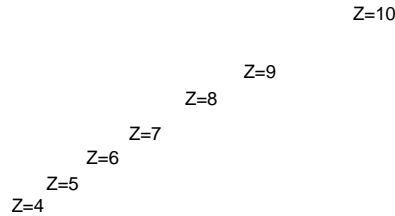


Figure 8: Fragmentation of ^{20}Ne ions, measured with a $420\ \mu\text{m}$ thick diamond detector.

Within the limited Z -range measured, the pulse heights increase nearly proportional to Z^2 . The ratio of the pulse heights with $^{40}\text{Ca}/^{20}\text{Ne}$ equals 3.4 was found to be higher than the ratio expected from the Bethe Bloch formula which amounts to 2.6.

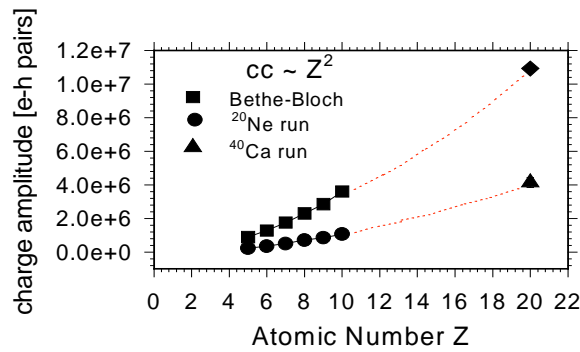


Figure 9: Z -dependence of the charge amplitude

This is an indication that the charge collection efficiency in diamond detectors improves with the ionisation density in the counter.

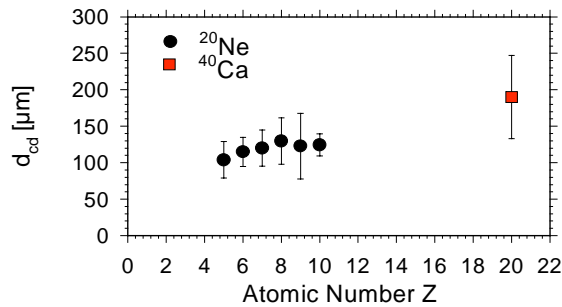


Figure 10: Z -dependence of the charge collection distance

This behaviour is the analogon to the "pumping" of the diamond detectors observed with γ -rays or ^{90}Sr -electrons (see 2.3.). A fast filling of the diamond traps occurs due to the leading charge of the high density plasma produced in the particles track. The mean free path of the charge carriers in the diamond

bulk increases. In Figure 10 the data taken in the two first experiments are plotted as the collection distances d_{cd} versus the atomic number Z of the projectiles. An increase in the collection distance from $d_{cd}=100 \mu\text{m}$ for $Z=5$ to $d_{cd}=190 \mu\text{m}$ for $Z=20$ is visible.

4.2. Pulse-Height Measurements with Broad-Band Amplifiers

In heavy-ion measurements diamond detectors can be operated with fast broad-band amplifiers because of the huge amount of charge produced by the particles. The aim was to develop low-noise, high-speed electronics for heavy-ion applications including a wide range of charged particles from protons to uranium ions. A low noise, 50Ω , 3 GHz amplifier has been developed and successfully tested with α -particles, ^{12}C , ^{20}Ne , ^{58}Ni and ^{208}Pb ions last year [11]. The lowest energy measured with this fast amplifier is shown in Figure 11. The ^{241}Am - α -particles are absorbed in $12 \mu\text{m}$ diamond. The 5.5 MeV α -distribution is well separated from the electronic noise. The α -spectrum is measured with a $370 \mu\text{m}$ thick diamond detector using the amplifier mentioned above.

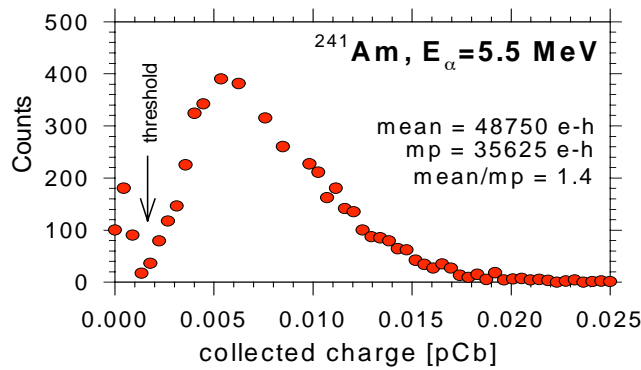


Figure 11: ^{241}Am α -spectrum measured with a $370 \mu\text{m}$ thick diamond detector. The electric field applied was $-1.4 \text{ V}/\mu\text{m}$, the broad-band amplifier used has a gain of 47 dB.

Lead-ion signals can be measured without any amplification. Figure 12 shows pulses produced from single ^{208}Pb ions at $1 \text{ GeV}/\text{amu}$ in a $265 \mu\text{m}$ diamond.

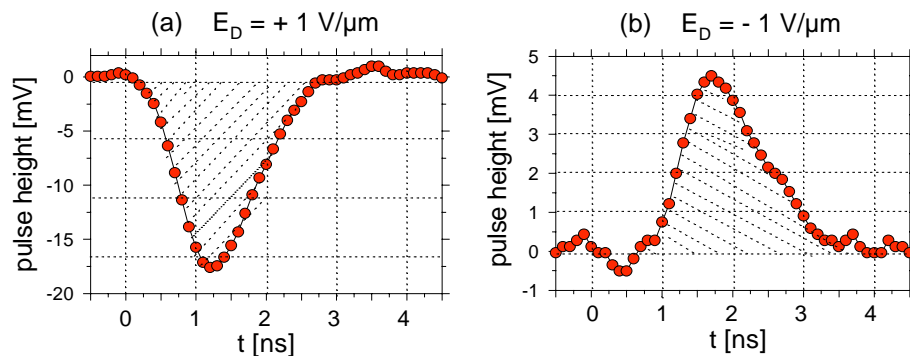


Figure 12: Diamond detector signals from ^{208}Pb ions at $300 \text{ MeV}/u$ without amplification

The signals correspond to an energy loss of 1.6 GeV . They are recorded and sampled with a digital storage sampling oscilloscope with a single-shot

sampling rate of 10 GS/s. The charge Q collected from thousand single ^{208}Pb ions is evaluated from the area of every single shot and is plotted in Figure 13. To compare our data with the results for minimum ionizing particles the same electric field of $\pm 1\text{V}/\mu\text{m}$ was applied to the detector. The electric field needed to achieve saturated charge-carrier velocities for $Z=82$ is by far not sufficient (see 3.). Consequently, the charge collection efficiency measured is lower than expected. Furthermore, in all spectra measured with heavier particles we observed a ratio mean/most probable value of 1.1 whereas the α -spectra show a more asymmetric shape with a ratio of 1.4.

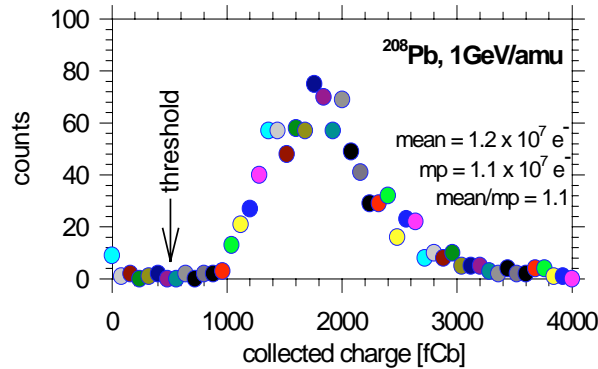


Figure 13: Pulse-height distribution of ^{208}Pb ions at 1 GeV/amu, measured with a 265 μm thick diamond detector without any amplification.

Applying a higher bias to the detector an improvement in the collected mean charge as well as a gaussian distribution with smaller FWHM is expected.

5. Time Measurements

The suitability of diamond detectors for heavy-ion time measurements was tested with uranium ions of 1 GeV/amu. Two diamond detectors with a thickness of 150 μm , followed by a silicon PIN-diode and a 350 μm thick plastic scintillator, were bombarded with uranium ions of 1 GeV/u. The TDC start was given by the plastic scintillator at the end of the setup. Figure 14 shows the time spectrum measured using 50 Ω , 1 GHz, Ortec 9306 amplifiers and extrapolating double-threshold discriminators, developed at GSI for the ultra-fast Pestov spark counters [12]. The observed intrinsic time resolution of $\sigma=39$ ps demonstrates the excellent timing properties of CVD diamond.

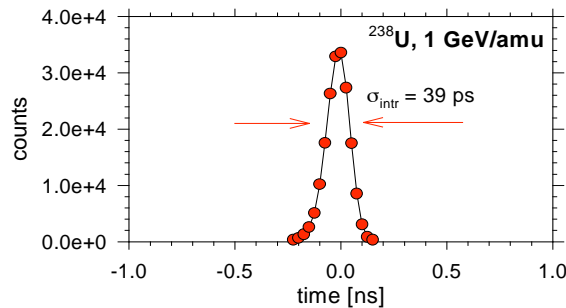


Figure 14: Time spectrum measured with two diamond detectors of a thickness of 150 μm

6. Counting-Rate Capability

To measure the rates expected from the high current injector of the SIS [11], signal widths in the order of 1 ns are needed. Whereas the rise time of the diamond signals measured is defined only by the bandwidth of the broad-band electronics used, the decay time is a convolution of both the mobility weighted carrier lifetime and the RC_D constant, given by the detector capacitance and the 50Ω impedance of the electronic system. Preliminary data from different samples tested show lifetimes of several hundred picoseconds. To maintain the short pulsewidth the detector capacitance has to be optimized by dividing the active area into strips or pixels. The capacitance of the diamond detector finally defines the counting rate capability.

Figure 15 shows data taken with a $265 \mu\text{m}$ thick single-channel diamond detector with a capacitance of 10 pF in a test performed with ^{20}Ne projectiles at 300 MeV/amu. Inside the SIS ring the beam intensity was measured with beam-current transformers and outside the SIS with an ionisation chamber in current mode, placed directly in front of the diamond detector.

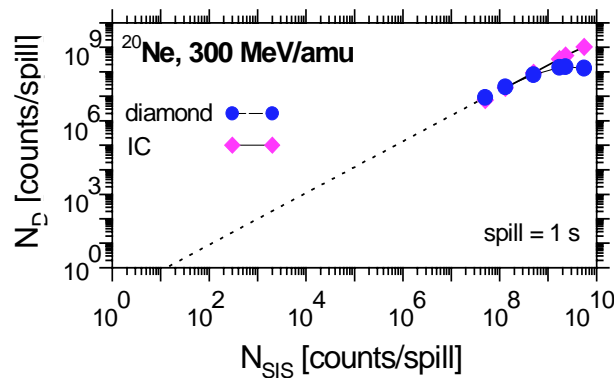


Figure 15: Beam monitoring, diamond in a single particle mode versus ionisation chamber integrating over the spill duration

Due to decay time contributions of transmission lines and the oscilloscope the final width of the signal was 3 ns. This led to unresolved single pulses in the spill and to counting losses for the intensities above 10^8 particles/s. However, the data demonstrate the ability of diamond detectors to measure efficiently heavy ion rates from single particles up to 10^8 particles/s. This rate can be further increased by a factor of 10 to 100 by dividing the detectors into strips or pixels.

7. First Applications

7.1. Beam diagnostics

Beam-intensity and beam-profile measurements are the first goals for beam diagnostic applications. Diamond detectors with an active area of $30 \times 30 \text{ mm}^2$ and a thickness of $350 \mu\text{m}$ metallized with strips respectively pixel electrodes of moderate pitch of about 3 mm are under development. Encouraged by the counting-rate tests performed so far the detectors are designed such that a

single diamond channel will be able to count a rate of at least 10^8 particles/s. With ten readout channels per diamond sample a total counting rate of 10^9 particles/s should be achievable.

Another possibility to reduce the large capacitance of thin diamond detectors is to apply interdigital electrodes with an interdigital pitch of a few millimeters. Different kinds of electrodes are presently been calculated, useful for beam monitoring in a non destructive mode.

Finally, the application of diamond detectors for high-frequency spill structure analysis [11] is also in preparation.

7.2. A Diamond Start Detector for HADES [13]

Diamond detectors show several advantages as start detectors for fixed-target heavy-ion experiments. They are radiation hard, they have a high counting-rate capability up to beam intensities of 10^8 particles/s and a uniform signal rise time below 500 ps. In the case of the HADES experiment the multiple scattering in a diamond start detector would be low compared to the scattering within the forseen heavy targets with thicknesses of several hundred micrometers. The background events produced from heavy projectiles in such detectors are strongly forward focussed and therefore not affecting the RICH [13].

To define the setup of the HADES start detector Monte-Carlo simulations are performed. ^{197}Au ions of 1 GeV/amu were focussed on a 1% interaction lenght ^{197}Au target with a total thickness of 300 μm [14]. Two identical diamond detectors with an octagonal shape (Figure 16) matching the beam spot at these locations are placed 75 cm upstreams, respectively 75 cm downstreams the target. The second detector shall veto all ions without reaction with target nuclei to provide a start signal at a rate of less than 10^7 particles/s.

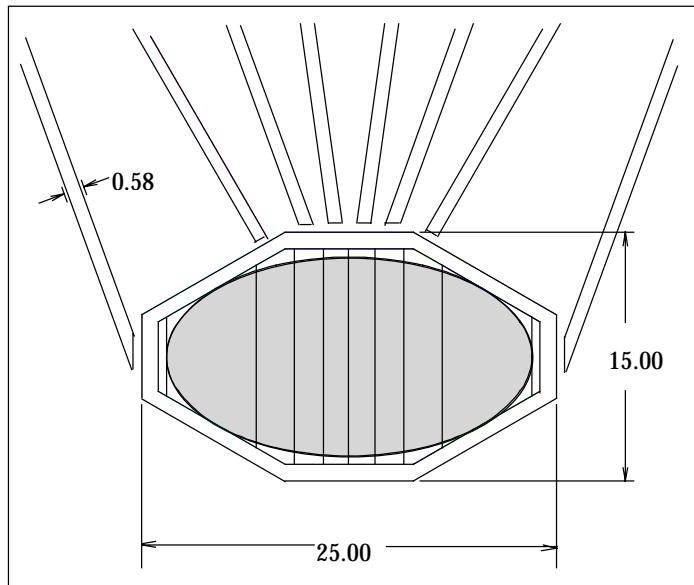


Figure 16: *First design of the HADES start detector*

Simulation results lead to two diamond detectors, which are divided in 8 strips of different width ranging from 5.4 mm down to 1.55 mm. The widths are optimized such that the count rate per strip is nearly constant. The octagonal shape reduces the capacitance of the outermost stripes by 40%. A coincidence with 3 opposite strips of the veto detector is sufficient to achieve a veto efficiency of 96.5%.

Special care has to be taken to maintain the narrow diamond pulse width and to minimize the deadtime of the fast electronics. While the amplifier used will be the GSI 3.5 GHz broad-band amplifier (see 4.2.) further in beam tests will be performed to select the best discriminator type for the expected narrow diamond signals. Depending on the quality of the diamond sample and the atomic number of the projectile the pulse-height resolution is in the order of 50%. Considering moreover the large dynamic range and the high multiplicity of events with $Z_1 \in [1, Z_{\text{proj}}]$ and $Z_2 = 1$ the type of discriminator to be used is not clear yet. Double-threshold discriminators [12] work excellently with diamond detectors (see 5.). The HADES collaboration will investigate in addition leading-edge discriminators as a second choice.

7.3. Heavy Ion Dosimetry

The sensors presently used for dosimetric measurements are ionisation chambers, silicon or natural-diamond detectors, respectively. They have an active volume of a few cubic micrometers only and have therefore to be displaced to cover larger volumes when verifying treatment planes. Furthermore, they measure the energy loss, out of which the applied dose is calculated.

It is expected that large area CVD-diamond pixel detectors will improve the accuracy of these measurements to $\pm 1\%$ and will significantly shorten the measuring time. Since single-particle counting is used, absolute dose measurements are possible.

8. Conclusions and Outlook

We have performed heavy ion measurements with diamond detectors of different quality and different thicknesses. Our results confirm so far the expectation that CVD-diamond is a very suitable detector material for intermediate and high energy heavy-ion measurements. The reason for this is on one hand the high amount of charge produced by the heavy ions and on the other hand the extremely high charge carrier velocity in the CVD-diamond material. The detectors provide fast collection of charge, the layers are homogeneous and the thicknesses vary from 30 μm to 2 mm. Common CVD material seems to be suitable for heavy ion measurements. Most applications do not necessarily require detectors of high quality material with long carrier lifetime. Laser cutting easily allows production of different shapes, thick-film photolithography structured electrodes and consequently position sensitive detectors with a spatial resolution of less than 50 μm [6].

The intrinsic time resolution of $\sigma = 39$ ps achieved with ^{238}U ions of 1 GeV/amu demonstrates the unique timing properties of CVD diamond. Due to the very small signal width high rates up to 10^9 particles/s can be measured. Finally, the poor pulse-height resolution remains the only disadvantage of today's CVD-diamond detectors.

Two important tests have to be performed in the next year. First, the Z^2 dependence of the diamond pulse-height has to be investigated systematically. The FRS spectrometer at GSI allows us to produce a wide range of fragments, identified in mass and charge for this purpose. Second, the radiation hardness studies of CVD-diamond under heavy-ion bombardment will be continued up to a fluence of 10^{13} to 10^{15} heavy ions/cm².

This work has been supported by the RD42 collaboration, of which GSI is a member since 1996.

References

- [1] G. Kraft et al., in *Hadron in Oncology*, eds. U. Amaldi and B. Larsson (Elsevier, 1994)
- [2] *Synthetic Diamond, Emerging CVD Science and Technology*, edited by Karl E. Spear and John P. Dismukes
- [3] S. Zhao, Ph.D. Thesis, The Ohio State University (1994)
- [4] S. M. Ryvkin, "Photoelectric Effects in Semiconductors", Consultants Bureau, New York (1964)
- [5] L. S. Pan, D. R. Kania, P. Pianatta, and O. L. Landen, *Appl. Phys. Lett.*, 57, 623 (1990).
- [6] D. Meier for the RD42 Collaboration, "5. Symposium on Diamond Materials", Electrochemical Society, Paris (1997)
- [7] E. Berdermann et al., GSI Scientific Report 1995, 1996, 1997
- [8] E. Berdermann et al., "5th International Conference of Advanced Technology and Particle Physics", Como (1996)
- [9] RD42 Status Report, CERN/LHCC 95-43
- [10] W. Dulinski et al., "Diamond Detectors for Future Particle Physics Experiments", CERN PPE/94-222, December 1994
- [11] P. Moritz et al., "Diamond Detectors for Beam Diagnostics in Heavy Ion Accelerators", DIPAC III, Frascati (1997)
- [12] C. Neyer et al., "A Precise Discriminator for Time-of-Flight measurements in ALICE", Proceedings of the first workshop on Electronics for LHC Experiments, Lisbon (1995)
- [13] R. Schicker et al., NIM A380 (1996) 586, and the HADES Proposal (1994)
- [14] W. Koenig, internal draft "The HADES Start Detector"